EuroRegio2016
June 13-15, 2016
Porto ▪ Portugal

Evaluation of the influence of the control strategy of the electric vehicle's motor on its radiated noise using 1D simulation

Gustavo Myrria[1], Fabien Chauvicourt[1] and Cassio Faria[1]

[1]Siemens Industry Software NV, Digital Factory – Product Lifecycle Management – Simulation and Test Solutions, Leuven, Belgium
gustavo.myrria@siemens.com, fabien.chauvicourt@siemens.com and cassio.faria@siemens.com

Abstract
The recent demands for reduction of greenhouse gases emission are pushing the automotive companies to develop alternative ways to provide mechanical power to vehicles. In this context, the electrification of the powertrain arose as an attractive option to replace the standard internal combustion engine. These vehicles acoustic signature is characterized by their tonal components which can disturb the passengers after a long exposure. To deal with this issue the modelling of the multiphysics nature of the noise generation in electrical machines must be taken into account: the modelling of the electromagnetic system to obtain the magnetic forces, the structural system to compute the forced response and the acoustic system to obtain the noise. Furthermore, in order to reduce the noise emission one can, among other methods, either try to reduce the magnetic force through the using of an appropriate control strategy, change the mechanical characteristics of the machine modifying the geometry or even its material properties. Thus, the objective of this work is to provide a fast way to compute the noise emitted by the electrical machine taken into account the physical systems involved and evaluating the influence of the control strategy on the noise inside the cabin. To accomplish this task, one dimension simulation was used to model the operation of the electric motor, the resulting vibration and the noise radiation. The influence of the control strategy on the total noise was evaluated through the using of different control strategies.

Keywords: Noise, Soft chopping, Hard chopping, 1D simulation, SRM.

PACS no. 43.50.+y, 84.50.+d, 46.40.-f

1 Introduction

Switched Reluctance Machines (SRM) have drawn attention in the recent years due to their characteristics and applicability in a wide variety of systems. According to Rabinovici [1], an intensive research on SRM began around twenty five years ago due to the progress in power electronics and microprocessors. The main advantages of SRMs are their simple and robust construction, possibility to work at very high rotational speeds, high mechanical torque at low speeds and simple power electronics driver. On the other hand, their main disadvantages are cumbersome control, relatively high torque ripple, mechanical vibrations and acoustic noise. Hence, because of the high acoustic noise emissions the Noise, Vibration and Harshness (NVH) is a concern for these machines and the mechanisms of the noise generation must be well understood in order to design quieter machines [2].

Due to their characteristics, a particular application for SRMs is to provide mechanical power electric vehicles (EV). Santos et al. [3] propose a multiphysics NVH modeling for the SRM using one dimensional (1D) simulation to obtain the electronic behavior of the SRM and a Finite Element (FE)

model to obtain the forced response and sound radiation. From this work one could perceive the resemblance of the current, acceleration and sound power level spectra. Though this approach is very powerful and obtained good results, it requires a significant amount of time to compute the result of the physical systems modeled by FE. Vlad et al. [4] compared the different current control techniques for a four phase SRM and evaluated their impact on the torque ripple. The authors have also investigated the impact of the hysteresis bandwidth on the torque ripple. They concluded the torque ripple is inversely proportional to the hysteresis bandwidth and the soft chopping suits better low frequency applications.
On the experimental side, the current control strategy impact on the noise and vibration has been studied by Sarrazin et al. [5] and more recently by Mollet et al. [6]. From these works can be noticed that hard chopping increased the loudness of the acoustic noise compared to soft chopping. Furthermore, the spectrum of the acoustic noise obtained by hard chopping excited a higher frequency region compared to soft chopping. Regarding to the origin of the acoustic noise generated by SRM, Cameron et al. [7] carried out tests on a SRM operating in different conditions and concluded that the radial force is the main vibration and noise source for these devices. Since there is a direct relation between the current applied on a phase and the respective radial force, a good choice of the current control strategy might lead to a quieter machine.

The objective of this work is to perform 1D multiphysical simulations of the SRM operation to determine the influence of the current control strategy on its NVH behavior. To achieve this goal, the hysteresis control strategies soft chopping and hard chopping were implemented on the SRM and their respective impact on the vibration and the sound radiation were obtained and discussed.

2 Materials and methods

The problem of the vibration and noise of SRM has a multi-domain characteristic and every physical system must be modeled in order to obtain a full representation of the system. This work proposes to model the SRM using a set of combined 1D sub-models. This approach is much faster compared to the current numerical methods. Figure 1 presents the methodology adopted and the relationship between the different physical systems.

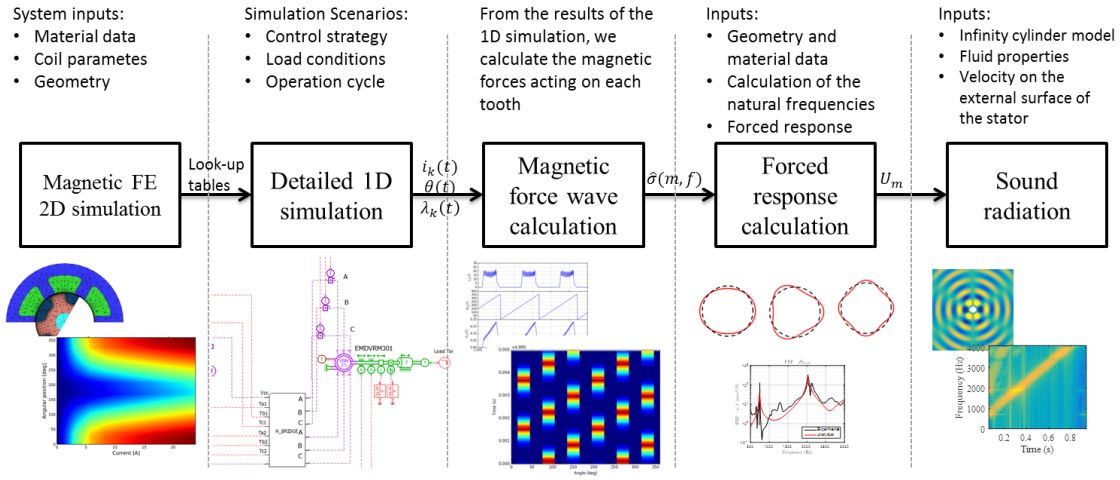

Figure 1 – Relationship between the different physical systems proposed in this work. Based on [3].

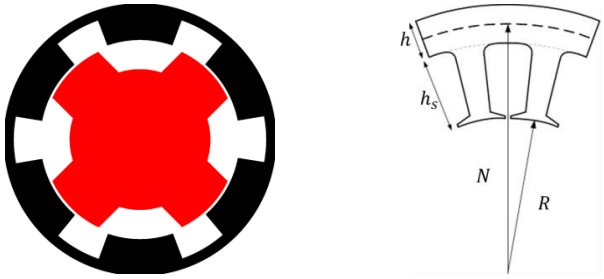

(a) (b)

Figure 2 – (a) 6/4 SRM machine modeled in this work and (b) the main geometric parameters used to model the machine.

2.1 Electric Model of the SRM

The SRM investigated here has 6 stator poles and 4 rotor poles and 3 phases controlled by an electronic system. As shown in the Figure 2, this machine has salient poles both for the stator and rotor. The information about the geometry and material properties of the SRM used here are shown in the Table 2.The DC wound windings are concentrated on the stator poles. The torque production of SRM is based on that a magnetic circuit tends to minimize its reluctance. Consequently, the rotor will turn towards a position where the reluctance of the excited phase is lower (or where the inductance L is higher). The position of the maximum inductance L_a is called aligned position (0 and 360 degrees), whereas the minimum inductance L_u occurs at the unaligned position (180 degrees). So, a proper commutation of the phases generates an overall torque on the rotor. The torque generated can be expressed in terms of co-energy W_{co} according to:

$$T(\theta, i) = \frac{\partial W_{co}(\theta,i)}{\partial \theta} \tag{1}$$

where θ and i are the angular rotor position and the phase current, respectively. Due to the fact that the SRM usually operates in deep saturation characteristics, linear representation cannot be used to model its behavior properly since it is not possible to state a linear relation between the torque and the phase current because of the strong non-linear behavior. An alternative commonly used to represent the non-linear behavior is to determine the variation of the flux linkage for the variation of the current and electrical angle through a numerical model. The resulted flux linkage is then stored in a look-up table and later used in a simpler analytical model. For the SRM investigated here, the flux linkage surface was obtained by a FE simulation done with the using of the commercial package JMAG and it is presented in the Figure 3.

Table 1 – Main mechanical characteristics of the stator.

Parameter		Value	Parameter		Value
External radius	R_c	0.102 m	Teeth mass	W_t	10 kg
Internal radius	R	0.075 m	Winding mass	W_g	2 kg
Mean radius	N	0.096 m	Yoke mass	W_y	3 kg
Length of the tooth	h_s	0.021 m	Young modulus	E	200 GPa
Length of the yoke	h	0.012 m	Mass density	ρ	7850 kg/m^3
Length of the stator	L	0.186 m			

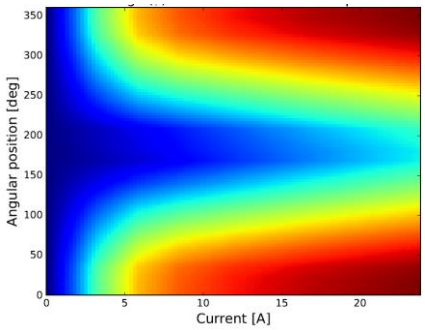

Figure 3 – Flux linkage of the SRM investigated in this work.

Once the flux linkage of a phase k is obtained (λ_k), the respective co-energy for this phase can be computed by the following expression:

$$W_{co,k} = \int \lambda_k(\theta, i)\mathrm{d}i. \tag{2}$$

The torque for this phase can be calculated from the expression Equation (1). The total torque can be obtained by the sum of the torque produced by each phase:

$$T = \sum_{k=1}^{n_p} T_k. \tag{3}$$

It is also interesting to notice the behavior of the voltage across the phase depending on the rotational speed of the rotor. The voltage on one phase can be deduced as follows [8]:

$$v = Ri + \frac{\mathrm{d}\lambda(\theta,i)}{\mathrm{d}t} = R_s i + L(\theta, i)\frac{\partial i}{\partial t} + \frac{\partial L(\theta,i)}{\partial \theta}\omega_m i \tag{4}$$

where L, R, ω_m are the inductance, resistance of the phase and the rotational speed of the rotor, respectively. The first term of the right-hand side of (4) represents the voltage drop on the phase resistance, the second corresponds to the induced voltage due to a variation of the phase current and the last corresponds to the back electromotive force (back-EMF). The SRM's control is often described in terms of "low-speed" and "high-speed" regimes. Low speed operation is typically characterized by the ability to arbitrarily control the current to any desired value. As the speed of the motor increases, it becomes difficult to regulate the current because of the increasing of the back-EMF and a reduced amount of time available for the commutation interval. A usual strategy to deal with this issue is to advance the firing angles in order to improve the characteristics of the SRM at high speed regime.

As observed from the Equation (3), the torque produced in these machines is strongly dependent on how the phases are excited. To prevent problems with the torque ripple the designer need to take care on the control system of the SRM. In order to evaluate how the controller impacts the NVH characteristics of the machine, the Hysteresis control is implemented with soft chopping and hard chopping, which will discussed with more details in the next section.

2.1.1 Hysteresis Controller

The role of the current controller block controls the signals provided to the power electronics converters. The converter used here is an asymmetrical H-bridge. There are three conduction modes generated depending on the states of the transistor switches, which are shown in Figure 4:

- When both switches T_1 and T_2 are ON, then the winding is in energizing mode;
- When both switches are OFF, then the winding is in de-energizing mode and
- When any one of the switches in ON and the other is OFF. Then the winding is in current regulation mode.

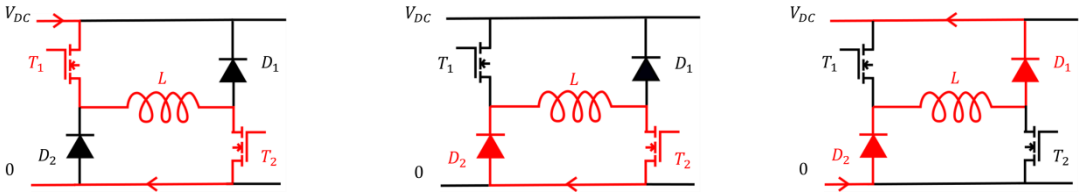

Figure 4 – Conduction modes of one phase depending of the states of the switches T_1 and T_2. (a) Energizing mode, (b) de-energizing mode and (c) regulation mode.

Depending on the way the switches are activated two different control strategies can be implemented on the SRM: soft chopping and hard chopping. For the soft chopping strategy, the Pulse Width Modulated (PWM) signal of the switch T_1 is made ON and OFF and the switch T_2 is maintained ON during the dwell angle interval. For the hard chopping strategy, both switches T_1 and T_2 are turned ON and OFF simultaneously. The choice of the control strategy used to activate the phase of the SRM impacts on the performance of the machine, as can be seen on Figure 5. For the lowest rotational speed plotted can be seen that the use of hard chopping strategy results in more ripples in the current signal compared to the soft chopping. As the rotational speed increases, the influence of the back-EMF becomes more significant and the results in a smoother current signal for both control strategy. The result of the flux linkage and the radial force for the phase follows the same behavior of the current.

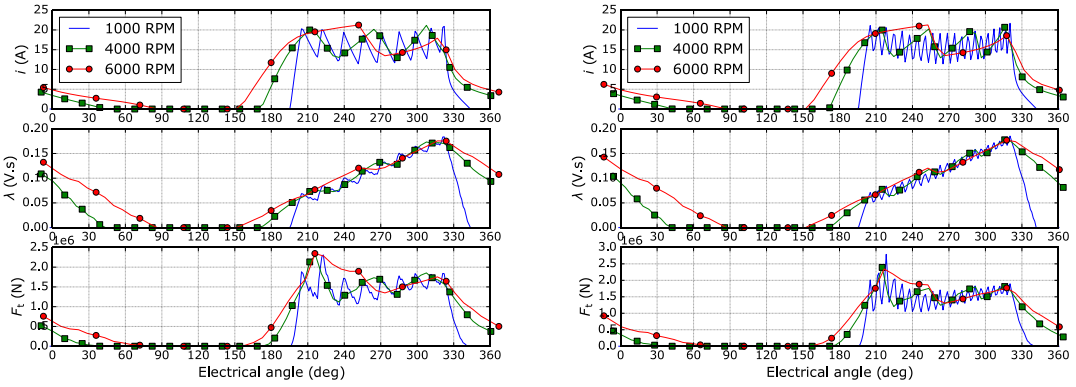

Figure 5 – Results of one phase of the SRM with soft and hard chopping for different speeds. One can notice the impact of the speed on the current wave and consequently to the flux linkage and the radial force on the tooth.

A closed-loop, speed controlled SRM drive is modeled and shown in Figure 6. The commercial software LMS Imagine.Lab Amesim was used to model and to run the simulation of the proposed

system. To assess the influence of the current control strategy on the NVH behavior of the SRM, soft chopping and hard chopping control strategies were used.

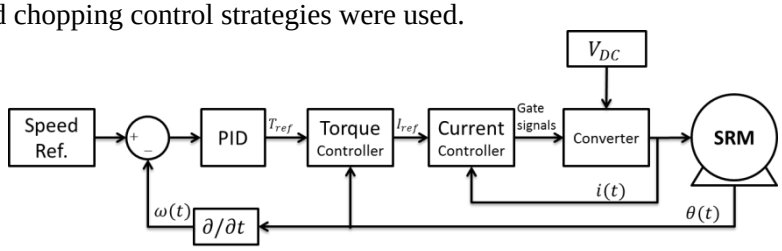

Figure 6 – Closed-loop control system of the SRM investigated in this work.

2.1.2 Magnetic Force wave on stator

Once all the results of the 1D simulation of the SRM operation were processed, the force wave acting on the stator can be obtained through the using of the Maxwell Stress Tensor. This radial force acting on a tooth (F_t) is obtained by the flux linkage acting on the respective phase of this tooth according to the expression below [8]:

$$F_t = \frac{\lambda_t^2}{2\mu_0 A_t} \tag{5}$$

where μ_0 and A_t are the magnetic permeability on vacuum and the overlap area between the rotor and stator pole, respectively. The flux on the tooth λ_t can be obtained by the instantaneous values of i and θ. By doing this calculation of each tooth the force wave on the stator can be obtained and then transferred to the structural system. Only the radial component of the magnetic force is considered in this analysis since it is the main source electromagnetic vibration and acoustic noise in SRM [9].

3 Results and discussion

After the processing of the full 1D multiphysical model introduced in the previous section, we will discuss the main obtained results in this section. Our focus is point out the impact of the control strategy on the vibroacoustic results. Furthermore, the performance of the machine on the electrical system is considered. Taking this as a starting point, Figure 7 shows the results of the current, average torque and magnetic radial force obtained by soft and hard chopping during the run-up simulation. During the run-up the acceleration was constant and the total signal duration was five seconds. The order lines can be easily distinguished from the spectrogram for both control strategies. Observing the spectrogram of the current of the phase A for soft chopping control strategy one can notice that the components with higher energy are encountered at frequencies less than 3 kHz. This behavior is particularly more pronounced for low speed regime. This result can be understood taking into account the result of the current profile shown in the Figure 5. In this figure one can notice that as the speed increases the shape of the current wave becomes smoother since the effect of the back-EMF is more significant with the increase of the speed. The torque results and the radial force on the tooth have a similar behavior to the one observed for the current, with higher amplitudes on frequencies lower than 3 kHz.

For hard chopping it can be observed a similar relationship between $i_A(s)$, $\tau(t)$ and $F_A(t)$ obtained by soft chopping. However, hard chopping control strategy resulted a current wave with more chops

during the dwell angle interval which impacts moving the harmonics components with high magnitudes to higher frequencies. From the spectrogram of these quantities it is clear that the hard chopping excited higher frequencies compared to the soft chopping. This can be not only harmful for the vibroacoustic behavior of the machine but also for the electric efficiency aspects since with more switches of the phases increases the power losses and can reduce the lifetime of electronic components [10]. With respect to the amplitude of the average torque and the radial force, a similar behavior obtained for the current was observed for these quantities. Moreover, significant amplitudes there exist for low and intermediate speeds in a profile in the form of an inverted C-shape and they are more prominent with the hard chopping. According to [5] it arises due to the commutation process.

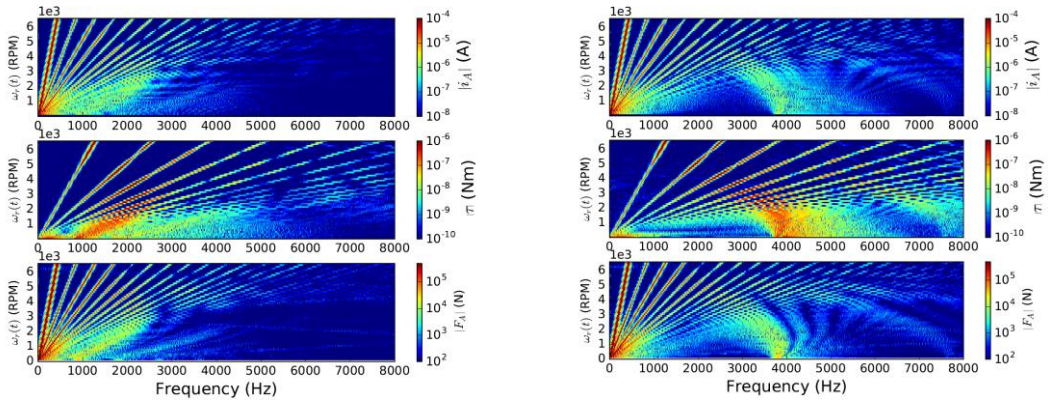

(a) (b)

Figure 7 – Results of current, torque and force on one phase of SRM with (a) soft and (b) hard chopping for run-up analysis.

The overall performance of the SRM for considering soft and hard chopping obtained by this 1D simulation is aligned to others experimental and numerical works [6, 3]. The prediction of the performance is vital for the prediction of the NVH outcome of the SRM due to the fact that the magnetic force wave is the most significant noise source during the operation of electric motors [7]. Furthermore, from the knowledge that the SRM are known by their high noise emission levels, this information is even more prominent.

From the presented modeling explained in the previous section, we computed the structural dynamics of the stator and later the forced response considering the force wave as the excitation. The natural frequencies are shown in the Table 2. In order to validate the analytical modeling an experimental modal analysis was performed on the stator. The test consisted to suspend the stator by very flexible strings to impose a free-free condition. Then, with the using of an LMS Qsources integral shaker a controlled force was imposed on the structure and the response vibration was measured on different positions on the external surface of the stator. From the results and with an appropriate post-processing the mode shapes and the respective natural frequencies can be determined. From the comparison of the results it can be concluded that the proposed analytical model for the stator was able to represent its structural behavior, with errors in the natural frequency prediction less than 3.5 %.

Imposing the magnetic force wave calculated for the SRM with soft and hard chopping on the structural model we computed the forced response of the stator. The results of the acceleration in a point on the external surface of the stator for soft and hard chopping control strategies are presented in the Figure 8 (a) and (b), respectively. In a first moment it is clear that the model could capture not only the forced response term but also the free response term of the vibration since the force is changing over the time. This behavior can be noticed on the spreader response of the acceleration observed on

the acceleration spectrogram. The order lines visible on the current and on the radial force on the stator pole are also present on the acceleration and their effect on the vibration is amplified on the natural frequencies of the stator. Hence, the natural frequencies and mode shapes of the stator plays a very important role on the final response of the stator. On the natural frequencies of the stator can be seen vertical lines on the spectrogram of the vibration, present due to the resonance phenomenon. The mode shapes excited were the mode $m = 0, 2$ and 4 at f =724, 3930 and 7484 Hz, respectively. The odd modes that there exist in this frequency range were not excited because the force wave has not energy on these modes due to its symmetry. Then, it is very important to take care on these even modes during the design stage since they are relevant on the NVH response of the SRM.

Table 2 – Comparison of the natural frequencies calculated by the methodology proposed by [11] with the results obtained experimentally.

Mode (m)	Frequency (Hz)		
	Analytical	Experimental	Δf_m (%)
0	7484	7235	3.4
2	724	732	1.1
3	2049	2050	0
4	3930	3906	0.6

The influence of the control strategy on the forced response can be observed on the spectrogram of the acceleration on a point of the stator subjected to the two magnetic force waves. The result of the SRM with hard chopping presented much higher amplitudes on the frequency range 4 kHz $< f <$ 8 kHz compared to the result with soft chopping. This is similar to the difference observed on the force wave spectrogram for these two control strategies. The result obtained with hard chopping was even worse due to the amplification of the response caused by the resonance between the force wave excitation and the mode shape $m = 4$ with a natural frequency equals to $f_4 = 3934$ Hz.

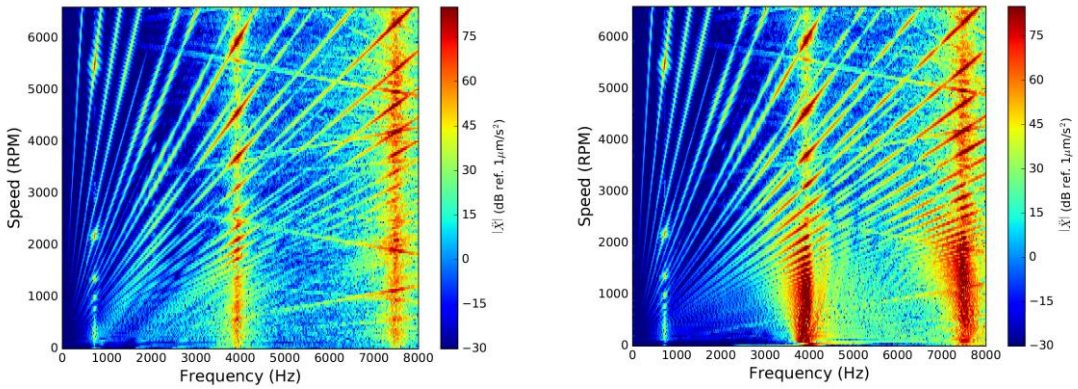

Figure 8 – Acceleration obtained during the run-up for (a) soft and (b) hard chopping.

The Sound Power Level (SWL) was calculated and the result for each control strategy is shown in the Figure 9. The A-weighting was added to the result of the SWL in order to take into account the transfer function of the human hearing system. The hard chopping resulted in higher noise emissions than the soft chopping, especially around the natural frequencies of the stator. Since soft chopping excites more low frequencies and the sound radiation has a behavior of a high pass filter, most of the contribution of this control strategy is filtered. This is not the case for the hard chopping once for this control strategy the most important components are encountered in high frequencies and are not filtered by the sound radiation characteristics of the structure. This result is important especially for SRM which are known to be noisy. For the control and the structural characteristics of the investigated

SRM the soft chopping has much lower noise emission than the hard chopping. Of course the parameters of the hard chopping can be changed in such way a better NVH behavior be met.

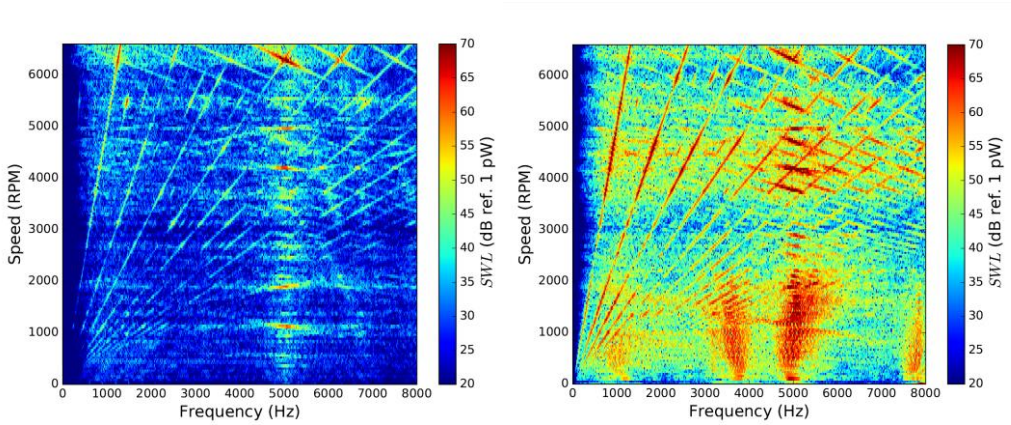

(a) (b)

Figure 9 – Sound Power Level computed by the 1D model for the SRM considering the (a) soft chopping and (b) hard chopping.

4 Conclusions

A complete 1D simulation of the SRM taking into account the different physical systems present during its operation was described and the results were discussed. Since the 1D simulation is much faster compared to the current numerical methods a variety of possibilities are opened such as optimization loops for instance. The control strategy for these machines was discussed and their impact on the NVH behavior of the SRM has been modeled and discussed. The soft chopping presented amplitudes with more energy for the electric current and the flux linkage in a single phase in lower frequencies compared to the hard chopping results. A similar behavior was observed for the radial force.

The forced response obtained by the hard chopping excited higher frequencies compared to the soft chopping. A care that must be taken into account by the designer is the resonance phenomenon. Since hard chopping excites higher frequencies it might excite a mode and cause high noise emissions. Moreover, hard chopping resulted in a significantly high vibration close to the natural frequency of the mode four. It is also observed that due to the symmetry the odd modes the force wave had not components for odd modes.

Finally, the sound emission for the SRM with hard chopping was significantly higher compared to the soft chopping. For soft chopping most of the energy was encountered at low frequency range and at this region the radiation efficiency of the stator is small. The result of the noise emission for soft chopping was even lower because of the A-weighting added the final SWL to represent the transfer function of the human hearing system. For the hard chopping the energy of the vibration was encountered in a region that the stator has better radiation efficiency and it reflected on the final radiation of the machine.

Acknowledgements

The presented research was performed in the context of the Marie Skłodowska-Curie Industry-Academia Partnerships and Pathways (IAPP) project “Design, Modelling and Testing tools for Electrical Vehicles” (DeMoTestEV).

References

[1] R. Rabinovici, "Torque ripple, vibrations, and acoustic noise in switched reluctance motors," *HAIT Journal of Science and Engineering B*, Vols. 2, Iss: 5-6, pp. 776-786, 2005.

[2] K. Kasper, M. Bosing, R. De Doncker, S. Fingerhuth and M. Vorlander, "Noise Radiation of Switched Reluctance Drives," in *Power Electronics and Drive Systems, 2007. PEDS '07. 7th International Conference on*, 2007.

[3] F. L. M. dos Santos, J. Anthonis, F. Naclerio, J. J. C. Gyselinck, H. V. der Auweraer and L. C. S. Góes, "Multiphysics NVH Modeling: Simulation of a Switched Reluctance Motor for an Electric Vehicle," *IEEE Transactions on Industrial Electronics*, vol. 61, no. 1, pp. 469-476, Jan 2014.

[4] P. Vlad, "Comparative Study of Different Current Control Techniques for a 4-Phase 8/6 Switched Reluctance Machine.," *Journal of Electrical \& Electronics Engineering*, vol. 4, 2011.

[5] M. Sarrazin, J. Anthonis, H. Van der Auweraer, C. Martis and J. Gyselinck, "Signature analysis of Switched Reluctance and Permanent Magnet electric vehicle drives," in *Electrical Machines (ICEM), 2014 International Conference on*, 2014.

[6] Y. Mollet, "Experimental Noise and Vibration Analysis of Switched Reluctance Machines - Comparison of Soft and Hard Chopping in Transient Conditions," in *ICRERA 2015: Proceedings of the 4th International Conference on Renewable Energy Research and Applications.*, 2015.

[7] D. Cameron, J. Lang and S. Umans, "The origin and reduction of acoustic noise in doubly salient variable-reluctance motors," *Industry Applications, IEEE Transactions on*, vol. 28, no. 6, pp. 1250-1255, nov/dec 1992.

[8] R. Krishnan, Switched Reluctance Motor Drives: Modeling, Simulation, Analysis, Design, and Applications, CRC Press, 2001.

[9] H. J. Zhang, C. Gao and S. H. Wang, "Analysis of radial force for switched reluctance motor," in *Applied Superconductivity and Electromagnetic Devices (ASEMD), 2013 IEEE International Conference on*, 2013.

[10] S. Kurian and N. G. K, "State of the art of switched reluctance motor for torque ripple minimization," *International Journal of Industrial Electronics and Electrical Engineering*, 2014.

[11] K. C. Maliti, "Modelling and analysis of magnetic noise in squirrel-cage induction motors," 2000.

[12] L. Cremer, M. Heckl and B. Petersson, Structure-Borne Sound: Structural Vibrations and Sound Radiation at Audio Frequencies, Springer Berlin Heidelberg, 2005.

[13] H. Jordan, Gerauscharme Elektromotoren: Larmbildung und Larmbeseitigung bei Elektromotoren, W. Girardet, 1950.

[14] C.-Y. Wu and C. Pollock, "Analysis and reduction of vibration and acoustic noise in the switched reluctance drive," *Industry Applications, IEEE Transactions on*, vol. 31, no. 1, pp. 91-98, jan/feb 1995.

[15] C. Faria F. Santos, F. Chauvicourt and Orlando, S., "Noise emissions on switched reluctance motors: evaluation of different structural models," in *EVS28 International Electric Vehicle Symposium and Exhibition*, 2015.